Available online at www.sciencedirect.com
SCIENCE DIRECT
Journal of Molecular Catalysis A: Chemical 242 (2005) 135–140
JOURNAL OF MOLECULAR CATALYSIS A: CHEMICAL
www.elsevier.com/locate/molcata

Synthesis of photocatalytic nanosized TiO_2–Ag particles with sol–gel method using reduction agent

Man Sig Lee [a], Seong-Soo Hong [b], Madjid Mohseni [a,*]

[a] *Department of Chemical & Biological Engineering, The University of British Columbia, 2216 Main Mall, Vancouver, BC, Canada V6T 1Z4*
[b] *Division of Applied Chemical Engineering, Pukyong National University, 100 Yongdang-dong, Nam-ku, Pusan 608-739, South Korea*

Received 17 January 2005; received in revised form 28 July 2005; accepted 28 July 2005
Available online 6 September 2005

Abstract

TiO_2–Ag nonoparticles were prepared with the sol–gel method using a reduction agent. The physical properties of the prepared particles were investigated by several characterization techniques. The major phase of all the prepared TiO_2–Ag particles was an anatase structure regardless of the $AgNO_3$ content. When the $AgNO_3$ content was 2 mmol/mol of TiO_2, the major phase (1 1 1) of silver could be clearly seen. The crystallite size of the TiO_2 particles calcined at 300 °C was 5–6 nm and that of the Ag particles increased from 10 to 15 nm with increasing $AgNO_3$ content. The high-resolution transmission electron micrographs (HR-TEM) showed that TiO_2–Ag nanoparticles possessed a spherical morphology with a narrow size distribution. The lattice fringe was 3.5 Å, which corresponds to the lattice spacing of (1 0 1) plane in the anatase phase. In addition, the presence of Ag in TiO_2–Ag nanoparticle prepared by the sol–gel method using a reduction agent improved the photodegradation of *p*-nitrophenol and the photocatalytic activity of TiO_2–Ag increased with the increase in the $AgNO_3$ content.

Keywords: TiO_2–Ag particles; Sol–gel process; Reduction agent; Photocatalytic degradation of *p*-nitrophenol

1. Introduction

Titanium dioxide, among the transition metal oxide semiconductors widely used in photocatalysis, is the most suitable photocatalyst due to its high photocatalytic efficiency and chemical and physical stability under the reaction conditions. However, there are still many challenges to be addressed for improving the photocatalytic activity of TiO_2. Because the semiconductor TiO_2 has a high band-gap ($E_g > 3.2$ eV), it is excited only by UV sources with wavelengths shorter than 388 nm in order to inject electrons into the conduction band and to leave holes in the valence band [1]. Thus, this practically limits the use of sunlight or visible light as an irradiation source in photocatalytic reactions on TiO_2. In addition, the high rate of electron–hole recombination on TiO_2 particles results in a low efficiency of photocatalysis. For the purpose of overcoming these limitations of TiO_2 as a photocatalyst, numerous studies have been recently performed to enhance electron–hole separation and to extend the absorption range of TiO_2 into the visible range. These studies include doping metal ions into the TiO_2 lattice [2], dye photosensitization on the TiO_2 surface [3], and deposition of noble metals [4]. In particular, noble metal-modified semiconductor nanoparticles have become the focus of many studies for maximizing the efficiency of photocatalytic reactions. The noble metals such as Pt [5] and Au [6] deposited or doped on TiO_2 have the high Schottky barriers among the metals and thus, act as electron traps, facilitating electron–hole separation and promoting interfacial electron transfer process [7].

Silver is particularly suitable for industrial applications due to its low cost and easy preparation. The effects of Ag dopants on the lattice or surface of TiO_2 have been examined [8,9]. TiO_2 loaded with silver enables the catalyst to perform

* Corresponding author. Tel.: +1 604 822 0047; fax: +1 604 822 5407.
E-mail address: mmohseni@chml.ubc.ca (M. Mohseni).

1381-1169/$ – see front matter © 2005 Elsevier B.V. All rights reserved.
doi:10.1016/j.molcata.2005.07.038

more effectively and shortens the illumination period [10]. He et al. [11] have investigated the effect of silver doping on the microstructure and photocatalytic activity of TiO_2 films prepared by the sol–gel method. It is found that suitable silver dopant can increase the activity and the mechanism is mainly attributed to the change of anatase grain size.

In this paper, nanosized TiO_2–Ag particles were prepared by a simple sol–gel method process using a reduction agent. The physical properties of the prepared particles were investigated by UV-DRS, X-ray diffractometer (XRD), energy-dispersive (EDS), and high-resolution transmission electron micrographs (HR-TEM). The effects of the $AgNO_3$ content on the physical properties of nanosized TiO_2–Ag particles and their impacts on the photocatalytic decomposition of a model compound, *p*-nitrophenol, were also studied.

2. Experimental

2.1. Synthesis of nanosized TiO_2–Ag

Nanosized TiO_2–Ag particles were prepared by a sol–gel process involving a reduction agent. Titanium tetraisopropoxide (TTIP, 98% Aldrich) and silver nitrate ($AgNO_3$, Aldrich) were used as precursors of titania and silver, respectively. Sodium citrate tribasic dihydrate ($C_6H_5Na_3{\cdot}2H_2O$, Aldrich) was used as a reduction agent, and water used in the experiments was doubly distilled and deionized.

$AgNO_3$ (1.0 and 2.0 mmol, respectively) was mixed with 500 mL of 4.0 mmol/L sodium citrate solution in a sealed four-way flask, and the reaction temperature was raised to 80 °C with continuous stirring. The color of the solution was observed to change from colorless to violet–brown indicating the reduction of silver. Then 1 mol titanium tetraisopropoxide and 0.15 mol HNO_3 were added to the solution, and the reaction was maintained at 50 °C for 24 h to obtain TiO_2–Ag sol. The prepared sol was dried at 105 °C for 1 day, and calcined in the range between 300 and 700 °C for 2 h in air.

2.2. Characterization of prepared TiO_2–Ag

The major phase of the synthesized particles was analyzed by an X-ray diffractometer (XRD) (Rigaku D/MAXIIC) using Cu Kα radiation. Crystallite size of the prepared particles was determined from the broadening of the anatase main peak at $2\theta = 25.3°$ by the Scherrer equation [12]. The prepared particles were dispersed in ethyl alcohol and then sonicated ultrasonically to separate out individual particles for the determination of the particle size. The particle size and external morphology of the particles were examined using an electron microscope (JEOL JEM 2020 200 kV electron microscope, $C_s = 0.5$ mm, point resolution of 0.19 nm) with a beryllium window energy-dispersive detector. In addition, the band-gaps of the prepared particles were obtained by the measurement of absorbance using a UV-DRS instrument (Varian Cary 100, Varian Inc.).

2.3. Photocatalytic reaction experiment

A biannular quartz glass photoreactor with the lamp immersed in the inner part was used for all the photocatalytic experiments (Fig. 1). The batch photoreactor was filled with 500 ml of an aqueous dispersion in which the concentrations of catalyst and *p*-nitrophenol were 1.0 and 50 mg/L, respectively. Continuous stirring maintained uniform concentration and temperature throughout the reactor. A 500 W high-pressure mercury lamp (Kumkang Co.) was used for the irradiation of the solution. The circulation of water in the quartz glass tube between the reactor and the lamp allowed cooling of the lamp and maintaining the reactor at the desired temperature. A mixture of oxygen and nitrogen (80% nitrogen and 20% oxygen) was used at a flow rate of 160 mL/min. Nitrogen was used as a carrier gas and pure oxygen was used to supply oxygen for the oxidation reaction. The samples were immediately centrifuged and the quantitative determination of *p*-nitrophenol was performed by a UV–vis spectrophotometer (Shimazu UV-240).

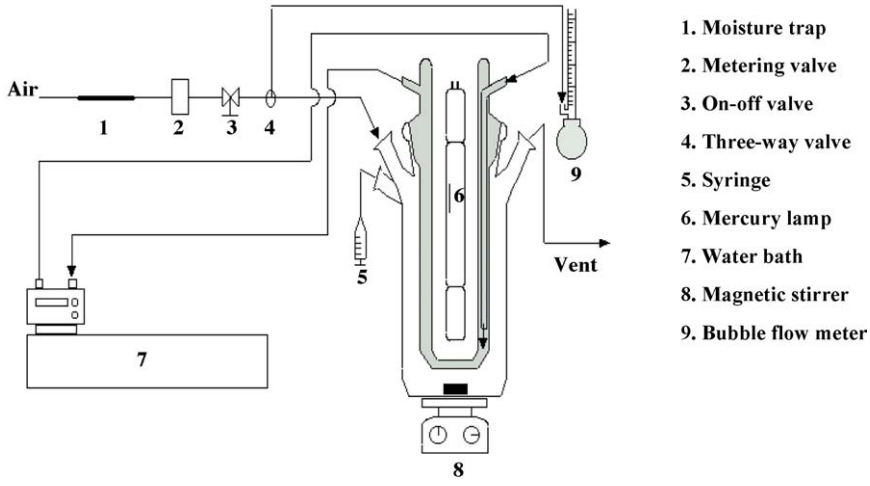

Fig. 1. Schematic diagram of the experimental apparatus for photocatalytic reaction.

3. Results and discussion

3.1. UV-DRS analysis

The nanosized TiO_2 and TiO_2–Ag sols synthesized in this experiment were transparent and stable for several months. Fig. 2(a) and (b) are the UV–vis spectra of the pure TiO_2 sol and Ag sol prepared, respectively, by the sol–gel method. Fig. 2(c) is the UV–vis spectra of the TiO_2–Ag 2 mmol sol prepared by the sol–gel method using a reduction agent. From Fig. 2(c), it can be seen that there is a framework silver species at 405 nm, indicating that the TiO_2–Ag particles were successfully prepared by the sol–gel method using sodium citrate as the reduction agent.

It is well known that the yield of photogenerated electron–hole pair depends primarily on the intensity of incident photons with energy exceeding or equaling the TiO_2 band-gap energy. The effect of silver addition on the band energy of TiO_2 was investigated with diffuse reflectance spectroscopy (DRS). The DRS of the pure TiO_2 and TiO_2–Ag particles calcined at 300 °C are shown in Fig. 3. Comparison of the diffuse reflectance spectra of the pure TiO_2 and TiO_2–Ag indicated that the band energy of TiO_2 for silver addition did not change and the band-gap of the particles was 3.1 eV. This suggested that the photocatalytic activity of TiO_2–Ag particles was not due to the change of the band energy of TiO_2.

3.2. X-ray diffraction analysis

The crystalline phase of the prepared nanoparticles were analyzed by XRD, and the results are shown in Fig. 4. These particles were only calcined at 300 °C for 2 h in air. The major phase of all the prepared TiO_2–Ag particles is an anatase structure regardless of the $AgNO_3$ content. When the $AgNO_3$ content was 2 mmol/mol of TiO_2, the major phase

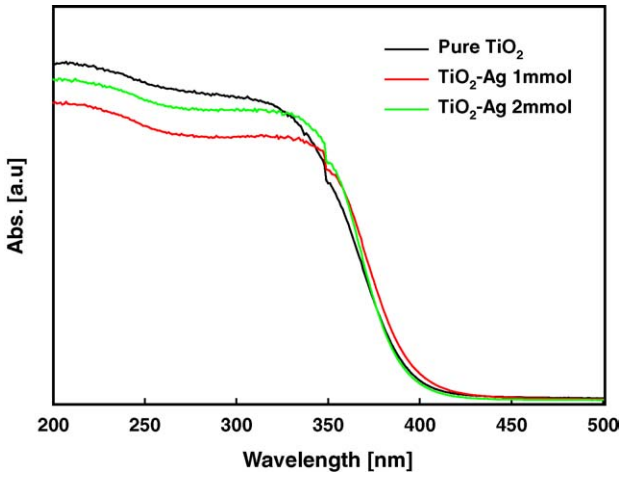

Fig. 3. Diffuse reflectance spectra of nanoparticles prepared at different conditions.

(1 1 1) of silver could be clearly seen, suggesting that the TiO_2–Ag nanoparticles were successfully prepared by this process involving the reduction agent. The crystallite sizes of the particles were determined from the broadening of the anatase main peak by the Scherrer equation [12]. The crystallite sizes of all the prepared particles were between 5 and 6 nm (Table 1). As shown in Table 1, the addition of $AgNO_3$ did not significantly affect the crystallite size of the particles.

Fig. 5 shows the XRD patterns of the TiO_2–Ag 2 mmol particles calcined at different temperatures. It is well known that calcination improves the crystallinity of the particles with the amorphous TiO_2 changing into the anatase phase and then the anatase phase changing into the rutile phase with increasing calcination temperature. It is reported that the transformation of the anatase phase into the rutile phase occurs at between 450 and 600 °C and that the transformation temperature depends on the kind of precursors and the preparation conditions and properties of the particles [13].

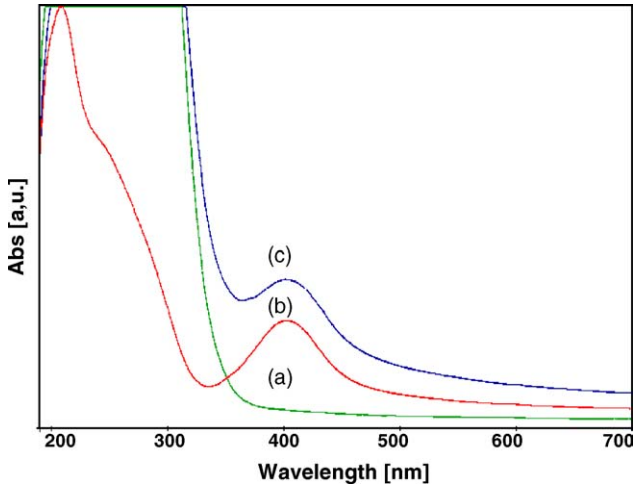

Fig. 2. UV–vis adsorption spectra of nanosol prepared at different conditions: (a) TiO_2 (b) Ag, and (c) TiO_2–Ag.

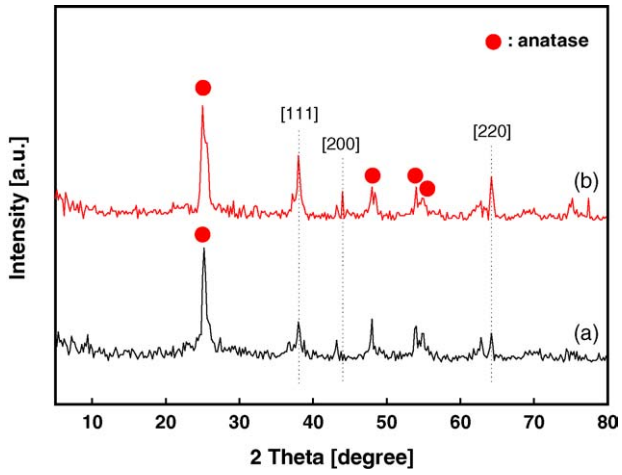

Fig. 4. X-ray diffraction patterns of TiO_2–Ag particles prepared at different $AgNO_3$ content: (a) TiO_2–Ag 1 mmol and (b) TiO_2–Ag 2 mmol.

Table 1
Characterization of nanoparticles prepared at different conditions

Catalyst[a]	XRD		TEM	Activity[d]
	Structure	Crystallite size[b] (nm)	Crystallite size[c] (nm)	k' (min^{-1}) × 10^{-2}
Pure TiO_2	Anatase	6	<5/–	1.8
TiO_2–Ag 1 mmol	Anatase–Ag	5	<5/10	2.9
TiO_2–Ag 2 mmol	Anatase–Ag	6	<5/15	3.4

[a] Calcinations temperature = 300 °C.
[b] Obtained by the Scherrer equation.
[c] Crystallite size of TiO_2 and Ag, respectively.
[d] Apparent first-order constants (k') of *p*-nitrophenol after 60 min irradiation.

As shown in Fig. 5, the particles calcined at 300 °C were identified as nanocrystalline anatase with the silver diffraction peak. With increasing calcination temperature to 500 °C, the silver diffraction (1 1 1) disappeared and the particles were identified as nanocrystalline anatase. Upon further increasing the temperature to 600 °C, the rutile peak appeared. It is thought that the silver species was covered by the crystals of TiO_2 that increased due to the high calcination temperature. The crystallinity increases with increasing calcination temperature because higher ordering in the structure of titania particles makes X-ray peaks sharper and narrower. The crystallite sizes of the particles prepared by different calcination temperatures are given in Table 2. It can be seen that the crystallite size of the anatase phase increased from 6 to 37 nm as the calcination temperatures increased from 300 to 700 °C. The size of rutile crystallites calcined at 600 °C was 47 nm and increased to 54 nm at 700 °C.

3.3. TEM analysis

Fig. 6(a) and (b) show the TEM micrographs of the nano-sized TiO_2–Ag particles prepared with different $AgNO_3$ contents and calcined at 300 °C for 2 h in air. The nanoparticles were spherical and had narrow size distribution. The crystallite size was determined (Table 1) by averaging the size of crystalline particles within the viewing area. The crystallite size of the prepared pure TiO_2 was 5 nm. The crystallite sizes calculated from XRD analysis were nearly the same as those obtained from TEM analysis. In addition, the crystallite size of Ag particles increased from 10 to 15 nm with increasing $AgNO_3$ content, which agreed closely with the results reported by Liu et al. [14]. Fig. 6(c) shows the lattice fringe of TiO_2–Ag 2 mmol nanoparticles. The lattice fringe, which has been used for phase determination show a value of 3.5 Å, corresponding to the lattice spacing of (1 0 1) plane in the anatase phase.

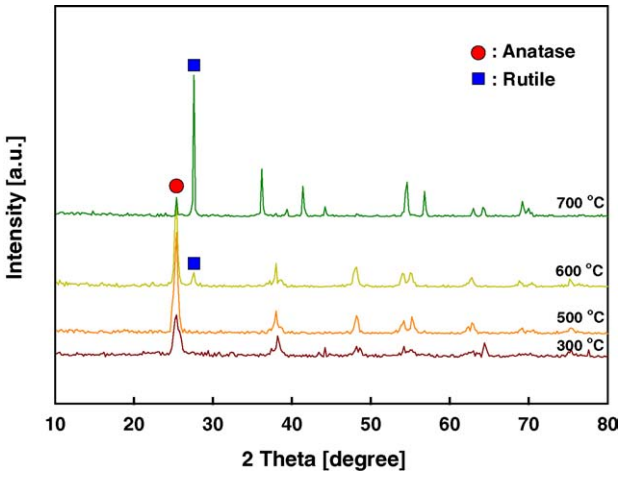

Fig. 5. X-ray diffraction patterns of TiO_2–Ag 2 mmol particles calcined at different temperatures.

Fig. 7 shows the EDS-pattern of TiO_2–Ag (2 mmol) particles in the HR-TEM mode from an area of 50 nm^2. The presence of four X-ray lines associated with O Kα, Ag Kα, Ti Kα, and Ni Kα is evident. Given that the Ni Kα line corresponds to the nickel grid used for TEM analysis, the results indicate that Ti, O and Ag are the constitutive elements of the nanoparticles prepared by the sol–gel method with different $AgNO_3$ contents.

3.4. Photocatalytic degradation of p-nitrophenol

The photocatalytic degradation of organic pollutants in water generally follows a Langmuir–Hinshelwood mechanism [15,16], with the rate being proportional to the coverage θ:

$$r = -\frac{dC}{dt} = k\theta = k\frac{KC}{1+KC} \quad (1)$$

where k is the true rate constant which is dependent upon various parameters such as the mass of catalyst, the flux of

Table 2
Characterization of TiO_2–Ag 2 mmol particles calcined at different temperatures

Calcination temperature (°C)	XRD		Activity[b]
	Structure	Crystallite size[a] (nm)	k' (min^{-1}) × 10^{-2}
300	Anatase–Ag	6	3.4
500	Anatase	15	4.6
600	Anatase/rutile	22/47	2.8
700	Anatase/rutile	37/54	1.6

[a] Obtained by the Scherrer equation.
[b] Apparent first-order constants (k') of *p*-nitrophenol after 60 min irradiation.

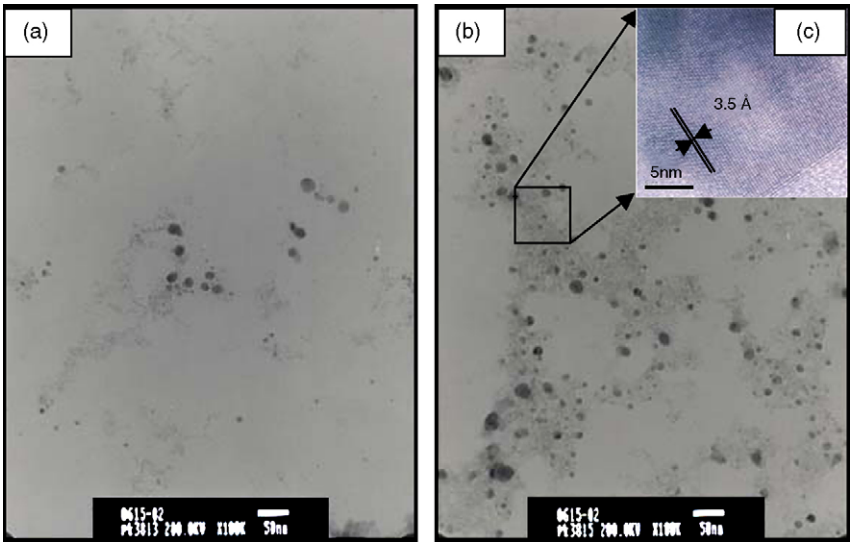

Fig. 6. TEM images of TiO_2–Ag particles prepared at different $AgNO_3$ content: (a) TiO_2–Ag 1 mmol; (b) TiO_2–Ag 2 mmol, and (c) lattice fringe of TiO_2–Ag 2 mmol.

efficient photons, the coverage in oxygen, etc., K the adsorption constant, t the time, and C is the concentration of organic pollutant (in this case, p-nitrophenol). For the low initial concentrations of pollutants, the term KC in the denominator can be neglected with respect to unity and the photocatalytic oxidation rate approaches first order:

$$r = -\frac{dC}{dt} = kKC = k'C \quad (2)$$

where k' is the apparent rate constant of the pseudo-first order kinetics. The integral form, $C = f(t)$ of the rate equation is:

$$\ln \frac{C}{C_0} = -k't \quad (3)$$

where C_0 is the initial concentration of p-nitrophenol.

The photocatalytic activities of nanosize TiO_2–Ag and TiO_2 particles for the decomposition of p-nitrophenol were examined and the results are shown in Fig. 8, as well as in Tables 1 and 2. The photocatalytic oxidation results were compared with those obtained from control experiments, involving no photocatalyst particles (data not shown). There was no significant removal of p-nitrophenol in the system when no photocatalyst was used in a control experiment. The apparent first order rate constant for the control test was more than one order of magnitude smaller than those obtained with the photocatalyst (presented in Fig. 8 and Tables 1 and 2). It is evident that the TiO_2–Ag particles had higher photoactivity than the pure TiO_2 and that the photocatalytic activity increased with the increase in the $AgNO_3$ content. More specifically, the photocatalytic activity of TiO_2–Ag (1 mmol) nanoparticles was about 60% higher than

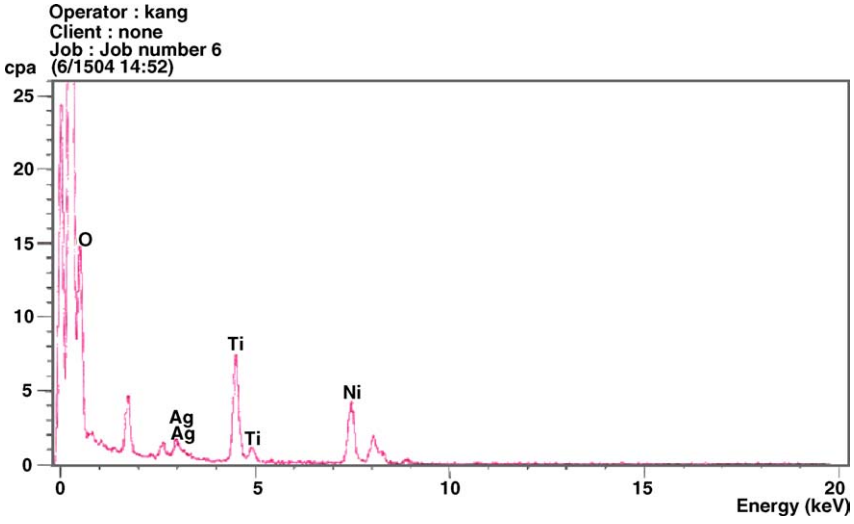

Fig. 7. EDS-pattern of TiO_2–Ag 2 mmol particles prepared by sol–gel method using reduction agent.

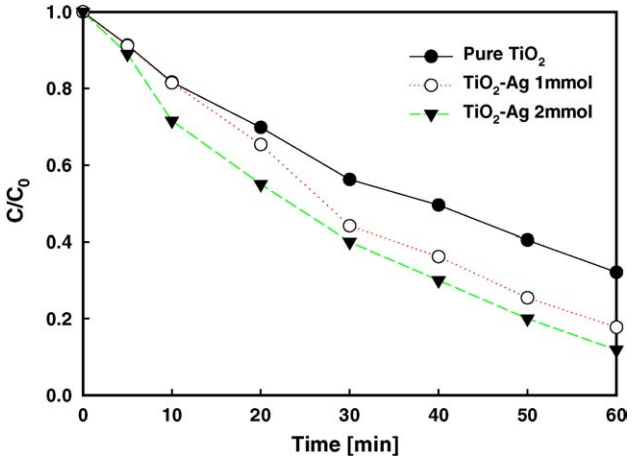

Fig. 8. Photodegradation of *p*-nitrophenol with pure TiO_2 and TiO_2–Ag nanoparticles.

that of the pure titania (Table 1). Statistical analysis of the apparent first order rate constants indicated that the higher activity of TiO_2–Ag photocatalyst was significant at 95% confidence intervals. From these results, it may be concluded that the presence of Ag in TiO_2–Ag particles prepared by the sol–gel method using a reduction agent has a positive effect on the photodegradation reaction of *p*-nitrophenol. Of course, it had been expected that Ag particles, deposited on the TiO_2 surface, as electron–hole separation centers [7,17], would have played important roles in the photocatalytic activities. This hypothesis was based on the fact that the electron transfer from the TiO_2 conduction band to silver particles at the interface is thermodynamically possible because the Fermi level of TiO_2 is higher than that of silver metals [8]. Such phenomenon would be expected to lead to the formation of Schottky barrier at metal–semiconductor contact region, which could improve the charge separation and consequently the photocatalytic activity of TiO_2.

The effect of calcination temperature on photocatalytic activities of TiO_2–Ag nanoparticles is presented in Table 2. Anatase-type titanium dioxide generally exhibits a higher photocatalytic activity than the other types of titanium dioxide (e.g. rutile) with regards to the decomposition of organic pollutants by suppressing the electron–hole recombination [18]. As shown in Table 2, the photocatalytic activity of the TiO_2–Ag particles calcined at 500 °C was the highest and decreased with increasing calcination temperature. In the case of titania particles calcined at 600 and 700 °C, the anatase and rutile phase were combined and the amorphous phase was mixed with the anatase phase, leading to the reduced photocatalytic activities and decomposition of *p*-nitrophenol.

4. Conclusions

TiO_2–Ag particles were successfully prepared by sol–gel process involving a reduction agent. The TiO_2–Ag sol synthesized was transparent and stable for several months. Comparison of the diffuse reflectance spectra of the pure TiO_2 and TiO_2–Ag indicated that the band energy of TiO_2 with silver addition did not change and the band-gap of the particles was 3.1 eV. The major phase of all the prepared TiO_2–Ag particles was an anatase structure regardless of the $AgNO_3$ content. When the $AgNO_3$ content was 2 mmol/mol of TiO_2, the major phase (1 1 1) of silver could be clearly seen. The crystallite size of TiO_2 particles calcined at 300 °C was 5–6 nm and that of Ag particles increased from 10 to 15 nm with increasing $AgNO_3$ content. The high-resolution transmission electron micrographs showed that TiO_2–Ag nanoparticles possessed a spherical morphology and had a narrow size distribution and the lattice fringe was 3.5 Å, which corresponds to the lattice spacing of (1 0 1) plane in the anatase phase. In addition, the presence of Ag in TiO_2–Ag particle prepared by sol–gel method using a reduction agent resulted in higher photodegradation of *p*-nitrophenol and the photocatalytic activity of TiO_2–Ag increased with increasing $AgNO_3$ content.

Acknowledgement

This work was supported by the Post-doctoral Fellowship Program of Korea Science & Engineering Foundation (KOSEF).

References

[1] C. Kormann, D.W. Bahnemann, M.R. Hoffmann, J. Phys. Chem. 92 (1988) 5196.
[2] S.D. Mo, L.B. Lin, J. Phys. Chem. Solids 55 (1994) 1309.
[3] K. Vinodgopal, D.E. Wynkoop, P.V. Kamat, Environ. Sci. Technol. 30 (1996) 1660.
[4] V. Vamathevan, R. Amal, D. Beydoun, G. Low, S. McEvoy, J. Photochem. Photobiol. A 148 (2002) 233.
[5] A. Sclafani, J.-M. Herrmann, J. Photochem. Photobiol. A 113 (1998) 181.
[6] V. Subramanian, E. Wolf, P. Kamat, J. Phys. Chem. B 105 (2001) 11439.
[7] J.-M. Herrmann, J. Disdier, P. Pichat, J. Phys. Chem. 90 (1986) 6028.
[8] K. Shiba, H. Hinode, M. Wakihara, React. Kinet. Catal. Lett. 64 (1998) 281.
[9] I. Ilisz, Z. Laszlo, A. Dombi, Appl. Catal. A 180 (1999) 25.
[10] M. Sokmen, A. Ozkan, J. Photochem. Photobiol. A 147 (2002) 77.
[11] C. He, Y. Yu, X.F. Hu, A. Larbot, Appl. Surf. Sci. 200 (2002) 239.
[12] B.D. Cullity, Elements of X-Ray Diffraction, second ed., Addison-Wesley, Reading, MA, 1978, p. 102.
[13] K.M. Reddy, C.V.G. Reddy, S.V. Manorama, J. Solid State Chem. 158 (2001) 180.
[14] S.X. Liu, Z.P. Qu, X.W. Han, C.L. Sun, Catal. Today 93–95 (2004) 877.
[15] C.S. Turchi, D.F. Ollis, J. Catal. 122 (1990) 178.
[16] G. Al-Sayyed, J.C. D'Oliveira, P. Pichat, J. Photochem. Photobiol. A 58 (1991) 99.
[17] A. Henglein, J. Phys. Chem. 83 (1979) 2209.
[18] A. Sclafani, L. Palmisano, E. Davi, New J. Chem. 14 (1990) 265.